Journal of Thermal Analysis and Calorimetry, Vol. 92 (2008) 1, 345–351

EVALUATION OF POZZOLANIC ACTIVITY AND PHYSICO-MECHANICAL CHARACTERISTICS IN CERAMIC POWDER-LIME PASTES

A. Bakolas, E. Aggelakopoulou and A. Moropoulou[*]

National Technical University of Athens, School of Chemical Engineering, Section of Materials Science and Engineering
9 Iroon Polytechniou St., 15773 Zografou, Athens, Greece

Ceramic powder has been used as an artificial pozzolanic addition, in preparing pozzolanic mortars for the historic/traditional structures' construction. In order to evaluate the pozzolanic activity of ceramic powder, several pastes were prepared, by mixing it with hydrated lime, in different ratios. The pastes were stored in standard conditions (RH=99±1%, T=25±1°C) and evaluated using thermal analysis (DTA/TG), X-ray diffraction (XRD), compressive strength tests and mercury intrusion porosimetry (MIP), in time. The obtained results revealed that the compounds formed were CSH and C_4ACH_{11} (monocarboaluminate) after 270 days of curing. The calcium hydroxide consumption increases as the initial amount of the ceramic powder in the paste augments. The maximum strength development is obtained for ceramic powder/hydrated lime ratio 3:1.

Keywords: *ceramic powder, hydrated lime, hydration phases, pozzolanic activity, thermal analysis*

Introduction

The type of mortar that is constituted of lime, ceramic fragments and/or ceramic powder and other stone aggregates was widely used since the Phoenician times to obtain hydraulic mortars [1–3]. This type of mortar presents different names depending on the historic era and the place that is met such as: Cocciopesto in Roman times, Horasan or Khorasan in Turkey, Surkhi in India and Homra in Arabic countries [2, 4]. Romans used this type of mortar in every part of their empire whenever natural pozzolanic materials were not available and the produced mortar should exhibit an advanced durability *vs.* severe climate and moisture conditions and high mechanical strength (aqueducts, thermal baths, foundations of buildings, bridges, etc.) [2, 5, 6].

Clay minerals, composed mainly by silica and alumina, present a sharp pozzolanic activity when heated at temperatures in the range of 600–900°C and ground in sufficient fineness. During the thermal treatment, silica and alumina loses the combined water, leading to a demolition of the crystalline network. Silica and alumina remain in an unstable amorphous phases that could react with hydrated lime and water, producing pozzolanic products [5].

The pozzolanic activity of a material is defined as its ability to react with portlandite ($Ca(OH)_2$), in the presence of water [7]. The pozzolanic activity of a ceramic powder depends on the chemical and mineralogical composition of the initial clay – a high content of clay favorise the pozzolanic activity – whereas the temperature and the duration of the thermal treatment – each clay presents an optimum firing temperature. Furthermore, the final characteristics of the ceramic powder that influences the pozzolanic activity are mainly the amorphous phase content and the specific surface area [8].

In this research work, in order to study pozzolanic activity of ceramic powder (CP), pastes produced with different mixing ratios of CP-lime were prepared and cured at 25°C, up to 270 days of hydration. DTA/TG and XRD analysis were used in order to define the compounds formed while the pastes' microstructure and mechanical characteristics were determined using mercury intrusion porosimetry and mechanical tests. The study of CP/lime system could provide us valuable information regarding the acquired mechanical strength and the hydration products formed addressed to historic buildings' restoration interventions.

Experimental

Materials and methods

The ceramic powder (CP) used for the preparation of CP/lime pastes is an artificial pozzolan produced by grinding handmade bricks baked at low temperatures (<900°C). The hydrated lime used is a commercial

* Author for correspondence: amoropul@central.ntua.gr

1388–6150/$20.00

Akadémiai Kiadó, Budapest, Hungary
Springer, Dordrecht, The Netherlands

Table 1 Chemical analysis and physical properties of materials used in pastes preparation

MT	SiO_2/	Al_2O_3/	Fe_2O_3/	CaO/	MgO/	K_2O/	Na_2O/	SO_3/	LOI/	dapp.	dreal	As
					%					g/cm^3	g/cm^3	m^2/g
L	0.17	0.18	0.07	70.06	2.35	–	–	0.77	25.60	0.50	2.34	13.60
CP	53.30	13.05	4.64	16.49	2.83	2.54	–	–	3.40	0.83	2.73	4.74

MT: material, LOI: loss of ignition, $d_{app.}$/g cm^{-3}: apparent density according to EN-45, d_{real}/g cm^{-3}: real density according to ASTM C-188-95, As/m^2 g^{-1}: specific surface area-BET method

product in a powder form that exhibits a $Ca(OH)_2$ content up to ~89%, and a relevant content of $CaCO_3$ ~5% (DTA/TG). Table 1 reports the chemical composition and the physical properties of the materials used for the pastes' preparation.

The grain size distribution of ceramic powder was determined by laser particle size analyzer (CILAS 715). It presents a sufficient fineness with cumulative passing percentage at 96 and 64 μm up to 100.0 and 95.9% correspondingly. X-ray diffraction analysis revealed that ceramic powder is comprised by quartz, ghelenite, wollastonite, anorthite, calcite and muscovite.

The pozzolanic activity of CP was determined according to EN 197-1 and EN 196-2 and the percentages of total silica and active silica were determined as 54.51 and 28.47%, respectively. Moreover, the pozzolanic activity of ceramic powder (according to Greek Presidential Decree 244/1980, article 8) is determined up to 6.2 MPa.

Table 2 Ratio of CP/L and water/(L+CP) (per mass) used for pastes preparation

Paste	CP/lime	Water/L+CP)
CP1	1	0.69
CP2	2	0.59
CP3	3	0.54

The mass ratio of the various solid components and the water to solid components ratio, employed in order to obtain the same consistency, for pastes' preparation are reported in Table 2. The mixing procedure was the same for all pastes: first, the amount of lime was mixed with the total amount of water, stirred for 3 min in a mixer. The ceramic powder was added gradually in the paste and stirred for other 20 min. The pastes were casted in cubic moulds of 2×2×2 cm and minicylinders (diameter: 2 cm, height: 4 cm [8, 9]) and stored in standard conditions (RH=99±1%, T=25±1°C). After 3 days of hydration the samples were demolded and stored in the same conditions until the testing date.

The following techniques were used for the evaluation of physicochemical and mechanical characteristics of pastes:

- Differential Thermal and Thermogravimetric Analysis (DTA/TG-Netzsch 409EP) in a static air atmosphere with heating rate of 10°C min^{-1} from ambient temperature up to 1000°C at 3, 7, 14, 28, 90 and 270 days of curing time, on ~100 mg of powder. The $Ca(OH)_2$ regarding the pozzolanic reaction products in time was determined. Prior to each collection of DTA/TG samples from the cube, the first 4–5 mm of the surface was removed by grinding, afterward they were placed in an oven at 60°C for 2 h and then in a desiccator for 1 h. Moreover, DTA/TG was performed on samples, obtained just after pastes' production, reported as 0 days.
- X-ray diffraction analysis (XRD, Siemens D-500) for the identification of crystalline compounds in pastes at different ages (0, 3, 7, 14, 28, 90 and 270 days). The preparation of XRD samples was the same as the DTA/TG one.
- Mechanical test (Wykeham Farrance, load cell: 50 KN, loading rate: 0.1 mm min^{-1}) performed in minicylinders, for the compressive strength and static modulus of elasticity determination, at 30 and 90 days of curing time.
- Mercury Intrusion Porosimetry (MIP, Fisons, Porosimeter 2000) for the microstructural characteristics determination at 90 days of curing time. Before each collection of MIP samples from the cube, the first 4–5 mm of the surface was removed by grinding and the samples were stored in a desiccator for 48 h.

Results and discussion

Differential thermal and thermogravimetric analysis (DTA/TG)

DTA curve of CP is shown in Fig. 1. An endothermic peak at ~720°C was observed noticed attributed to decarbonation of $CaCO_3$. Figures 2–4 report the DTA curves of CP1, CP2, CP3 pastes at 0, 3, 7, 14, 28, 90 and 270 days of curing. The main endothermic (endo) peaks are observed in the following temperature ranges:

- ~120°C (endo) Dehydration of CSH

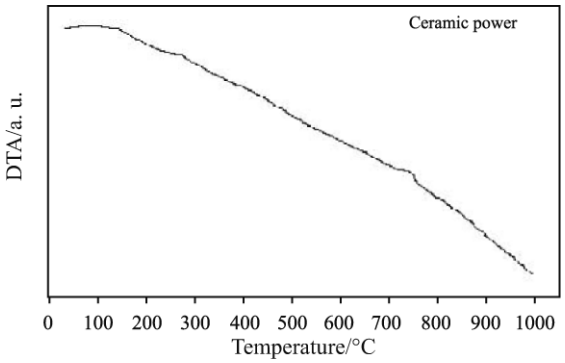

Fig. 1 DTA curve of CP

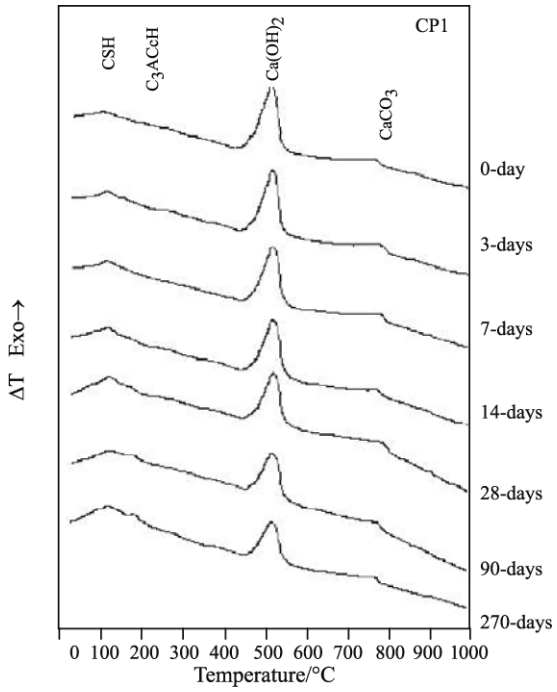

Fig. 2 DTA curves for CP1

- ~180°C (endo) Dehydration of $C_4A\overline{C}H_{11}$($3CaO\cdot Al_2O_3\cdot CaCO_3\cdot 11H_2O$, monocarboaluminate
- ~500°C (endo) Dehydration of $Ca(OH)_2$
- ~780°C (endo) Decarbonation of $CaCO_3$

It should be noticed that the peaks attributed to the dehydration of CSH and monocarboaluminate are firstly detected for all pastes at the period of 7–14 days with increased intensity from 14 days until 270 days. On the other hand the peaks related to $Ca(OH)_2$ and $CaCO_3$ are decreasing slightly until 270 days.

Regarding the endotherm at 180°C, two phenomena could occur at the same time: the dehydration of gehlenite hydrate (C_2ASH_8) along with the dehydration of monocarboaluminate ($C_4A\overline{C}H_{11}$). Taking into account that XRD analysis revealed only the presence of C_4ACH_{11}, the exothermic peak could

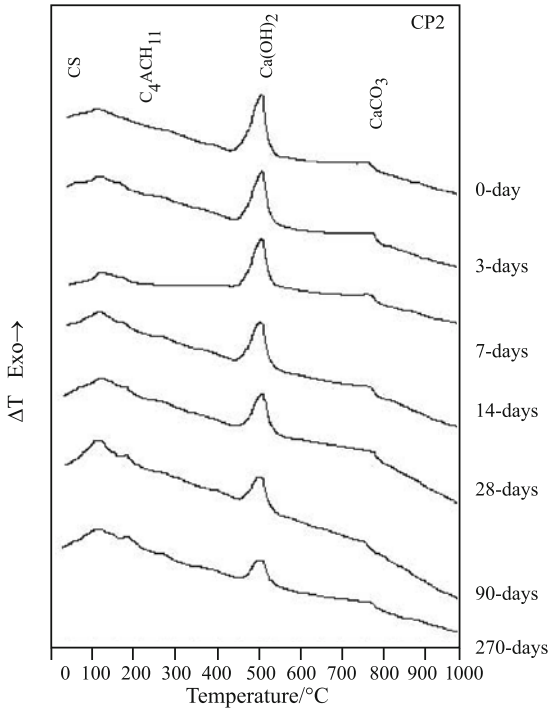

Fig. 3 DTA curves for CP2

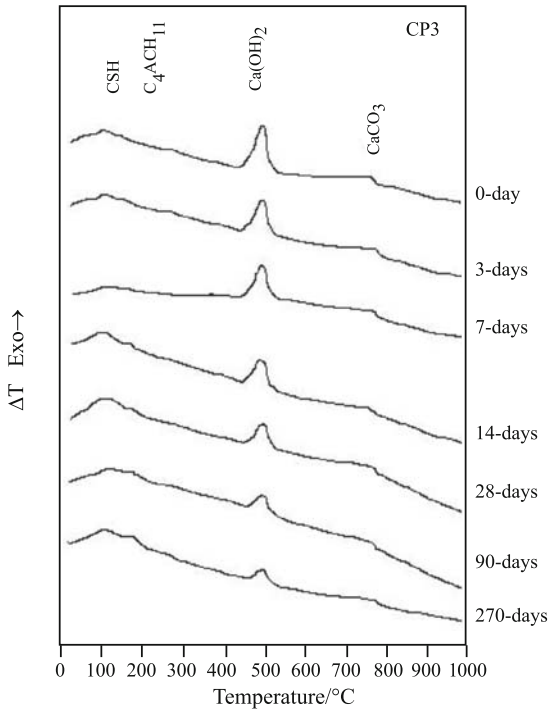

Fig. 4 DTA curves for CP3

be attributed to monocarboaluminate as a product of reaction between ceramic powder and hydrated lime. Monocarboaluminate was also detected in the historic mortars of Hagia Sophia (where ceramic powder was used as an artificial pozzolan) after thousands of years of their production, by using Neutron Diffraction Pattern [10].

The intensity of the endotherm attributed to $Ca(OH)_2$ (CH) dehydration is reduced, with time, while for all pastes the free CH is not consumed at 270 days.

By using the 2nd derivative of TG and DTA analysis [11] the mass loss (%) of the chemical compounds detected in pastes are calculated and presented in Figs 5–7 for CP1, CP2 and CP3 respectively, *vs.* curing time. All pastes present low percentage of physically absorbed water (calculated from 25 up to 100°C), less than 1%.

In addition, for all pastes, the observed mass loss attributed to dehydration of CSH (calculated from 100°C to the end of phenomenon) is formed at 0 days and exhibits a maximum value at the time period of 14–270 days.

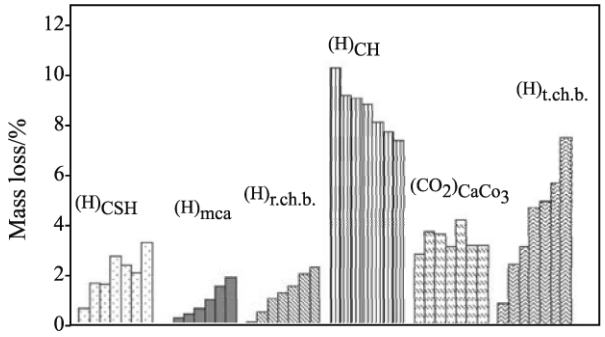

Fig. 5 Mass loss (%) of the compounds detected in CP1 paste, at 0, 3, 7, 14, 28, 90, 270 days of curing time

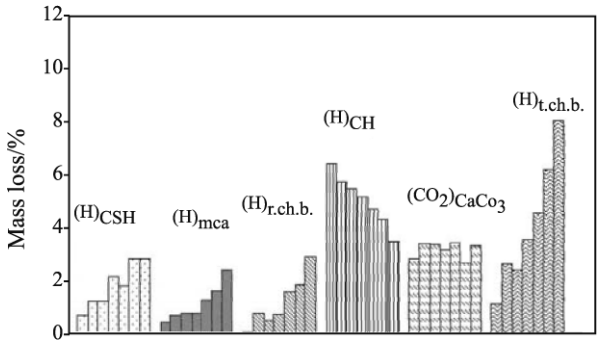

Fig. 6 Mass loss (%) of the compounds detected in CP2 paste, at 0, 3, 7, 14, 28, 90, 270 days of curing time

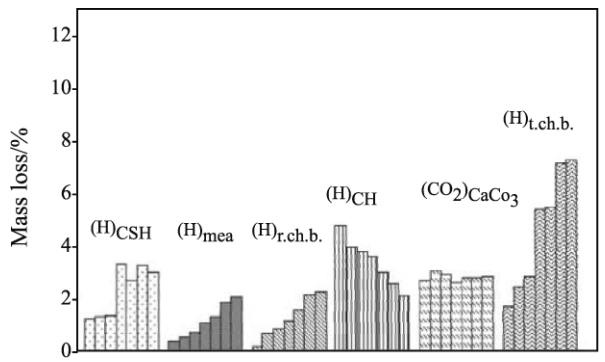

Fig. 7 Mass loss (%) of the compounds detected in CP3 paste, at 0, 3, 7, 14, 28, 90, 270 days of curing time

Mass loss concerning the $C_4A\overline{C}H_{11}$ ($(H)_{mca.}$), presents an increase until 270 days of curing time where the maximum value is detected. Moreover, the mass loss attributed to the residual chemically bound water ($(H)_{r.ch.b.}$) is calculated from the end of monocarboaluminate dehydration up to the beginning of calcium hydroxide dehydration [12].

The mass loss of the total chemically bound water ($(H)_{t.ch.b.}$) is calculated according to the equation:

$$(H)_{t.ch.b.} = (H)_{CSH} + (H)_{mca} + (H)_{r.ch.b.}$$

$(H)_{t.ch.b.}$: total chemically bound water, calculated in the temperature range ~100–460°C, $(H)_{CSH}$: chemically bound water of CSH, calculated in the temperature range ~100–160°C, $(H)_{mca}$: chemically bound water of monocarboaluminate, calculated in the temperature range ~160–230°C, $(H)_{r.ch.b.}$: residual chemically bound water, calculated in the temperature range ~230–460°C.

The values of $(H)_{r.ch.b.}$ and $(H)_{r.ch.b.}$ present an increasing trend with curing for all pastes, although such values are much more lower than the relevant values of metakaolin/lime pastes, indicating that ceramic powder/lime pastes present lower values of total chemical bound water and therefore lower values of pozzolanic products than metakaolin/lime pastes [8].

The mass loss attributed to the chemically bound water of CH is decreasing until 270 days of curing time, whereas a fraction of free lime remain in all pastes until the end of curing time, indicating that free lime was not fully consumed.

The mass loss ascribed to $CaCO_3$ present insignificant variations in time.

For all pastes, the total chemically bound water values present an increase until 270 days of aging. Furthermore, taking into account the TG results, the percentage of consumed $Ca(OH)_2$ ($(CH)_{cons.}$ (%)) is determined according to the equation [13, 8]:

$$(CH)_{cons.}(\%) = 100\frac{(CH)_0 - (CH)_t}{(CH)_0}$$

where $(CH)_{cons.}$ (%): consumed CH (%) at a specific age (t), $(CH)_0$: the initial amount of CH in the lime-ceramic powder paste, $(CH)_t$: the amount of CH in the paste for a specific age (t).

Figure 8 presents $(CH)_{cons.}$ (%) *vs.* curing age for CP1, CP2, CP3 pastes. From the results, it is noticed that the highest rate of CH consumption is reported for CP3, followed by CP2 and CP1. The $(CH)_{cons.}$ (%) at 270 days is about 56, 46 and 28% for CP3, CP2 and CP1 respectively.

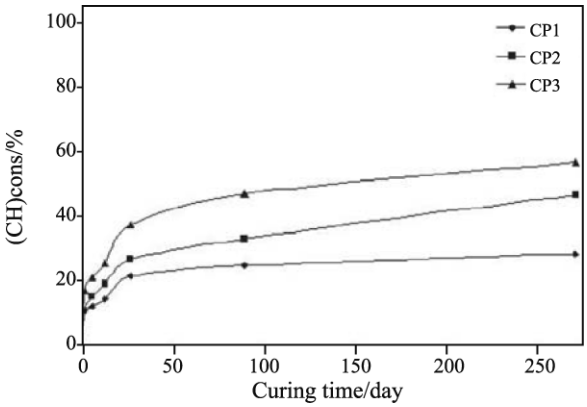

Fig. 8 Consumed CH (%) in time for CP1, CP2, CP3

X-ray diffraction analysis (XRD)

Figure 9 illustrates the XRD patterns for CP pastes in different time intervals. At 0 days, the patterns of portlandite (P) and calcite (Cc) are noticed, attributed to the presence of lime in pastes. Furthermore, quartz, anorthite, ghelenite and wollastonite are detected, attributed to ceramic powder. The intensity of the compounds is, slightly, decreased with time, as the reaction among lime and ceramic powder is taking place. In all pastes, the patterns of lime are detected at 270 days, indicated that free lime is not consumed even at 270 days of curing time. This fact is in accordance with DTA/TG results.

The patterns of C_4ACcH_{11} as a hydrated product of pozzolanic reaction that took place between ceramic powder and hydrated lime, has been detected by XRD. It was initially observed after 14–28 days for all pastes, with increasing intensity with time. The intensity of C_4ACcH_{11} exhibited a more intense peak in the case of CP2 paste. Monocarboaluminate (C_4ACH_{11}) is revealed beyond 28–14 days of curing time, as a result of reaction between CH, alumina and silica [8, 14].

In addition, CSH as a pozzolanic product is hardly detectable by X-ray analysis, due to its low degree of crystallinity. Nevertheless, in diffractograms of all pastes obtained, a wide band of peaks appears in the range of 2θ 28–31° [8, 15], after 3–7 days, attributed to the presence of CSH.

Mechanical tests

Table 3 presents the values of compressive strength performed on minicylinders (mean value of three measurements) as far as the values of static modulus of elasticity, calculated at 40% of the compressive strength (tangent E_{st}). Standard deviations of the three measurements are reported as well.

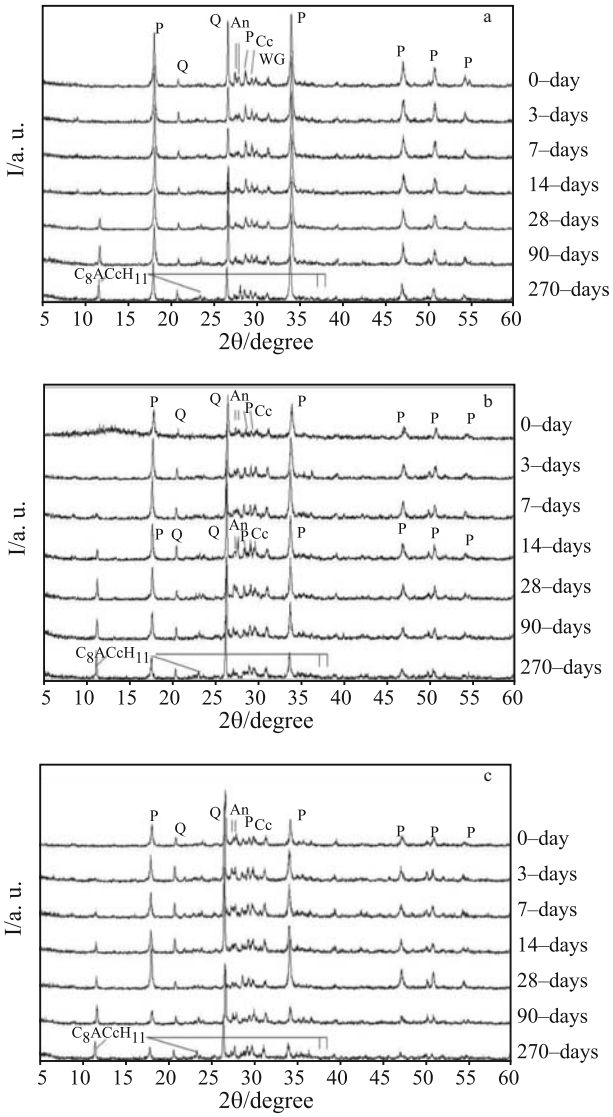

Fig. 9 XRD patterns for CP/lime pastes at 0, 3, 7, 14, 28, 90, 270 days of curing time a – CP1, b – CP2, c – CP3 (P: portlandite, Cc: calcite, An: anorthite, G: ghelenite, W: wollastonite)

According to the obtained results, CP3 presents the highest values of compressive strength, followed by CP2 and CP1. Mechanical strength is increased slightly from 30 to 90 days for all pastes. This is in accordance with the values of total chemically bound water that increases for all pastes until 270 days of curing time (TG data). Static modulus of elasticity displays a similar trend with compressive strength with maximum value reported for CP2 and CP3 pastes. Comparing the results of DTA/TG with those of mechanical tests, it could be deduced that pastes presenting a high percentage of total chemically bound water (CP2, CP3) (attributed to the hydrated products), exhibit high values of compressive strength and static modulus of elasticity.

Table 3 Compressive strength and static modulus of elasticity for CP/lime pastes, at 30 and 90 days of curing time

Paste	Time/ day	Fc/ MPa	SD	Est./ MPa	SD
CP1	30	1.2	0.1	121	13
	90	3.0	0.1	136	14
CP2	30	2.1	0.4	129	12
	90	4.4	0.7	156	41
CP3	30	2.9	0.1	113	22
	90	5.4	0.2	145	31

Fc (MPa): compressive strength, Est. (MPa): static modulus of elasticity, SD: standard deviation

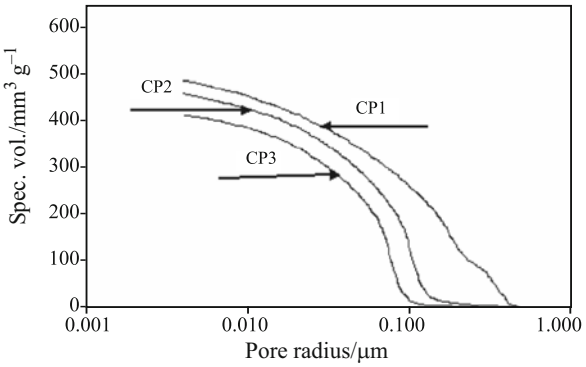

Fig. 10 Distribution of specific volume (mm^3 g^{-1}) to the pore radius

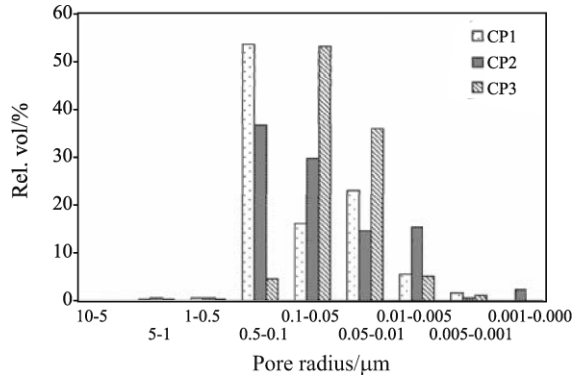

Fig. 11 Distribution of relative volume (%) in different ranges of pore radius

Mercury Intrusion Porosimetry (MIP)

Table 4 reports the microstructural characteristics of pastes (mean values of three measurements) at 90 days of curing time. It was observed that the pore radius average presents the same values for CP2 and CP3, whereas CP1 exhibits higher one. As the ratio of CP/lime increases, the open total porosity decreases. Similar trend is observed for corrected bulk density and total cumulative volume of pastes. Regarding the specific surface area, it presents almost the same values for all pastes.

Figure 10 presents the distribution of specific volume (mm^3/g) to the pores radius of pastes where a different distribution could be noticed. CP1 exhibits a distribution shifted to coarser pores. Furthermore, as the CP/lime ratio increases, there is a clear shift to narrower pores. The curves correspondent to CP1 and CP2 present a slightly increasing trend, due to the presence of narrower pores, beyond the detection limit of the instrument. In the case of CP3, the slope of the curve remains rather stable.

Figure 11 presents the percentage of relative volume in different ranges of pore radius. It could be noticed that the higher percentage of relative volume for pastes CP1 and CP2 is distributed in the range of pore radius 0.5–0.1 μm whereas for paste CP3 the higher percentage of relative volume CP2 is distributed in the range 0.1–0.05 μm.

More specifically, the ~53 and ~37% of the relative volume is distributed in pore range of 0.5–0.1 μm, for CP1 and CP2. In the case of CP3, the percentage of relative volume ascribed to pores in the range 0.1–0.05 μm arises up to ~53%.

Conclusions

From the aforementioned results the following conclusions could be obtained:

- DTA and XRD data revealed that the compounds formed during the pozzolanic reaction in CP/lime pastes are: CSH and $C_4A\overline{C}H_{11}$.
- Regarding the lime consumption, the initial amount of calcium hydroxide is not consumed after 270 days of curing for the ceramic powder/lime pastes examined. As the mixing ratio of ceramic powder/lime is increasing the total percentage of consumed lime is increasing as well.

Table 4 Characteristics of pastes microstructure at 90 days of curing time as determined by Mercury Intrusion Porosimetry

Paste	T.C.V./mm^{3}g^{-1}	As/m^2 g^{-1}	P.R.A./μm	dbulk/g cm^{-3}	dbulk.cor./g cm^{-3}	O.T.P./%
CP1	507.89	27.22	0.18	1.14	2.72	57.94
CP2	431.99	28.23	0.07	1.25	2.73	54.13
CP3	415.23	26.70	0.07	1.26	2.64	52.31

T.C.V.: total cumulative volume (mm^3/g), As: specific surface area (m^2/g), P.R.A.: pore radius average (μm), dbulk: bulk density (g/cm^3), dbulk.cor.: corrected bulk density (g/cm^3), O.T.P.: open total porosity (%)

- Mechanical strength is increased slightly from 30 to 90 days for all pastes. Static modulus of elasticity displays similar trend. The maximum value of compressive strength and static modulus of elasticity is reported for paste prepared by mixing hydrated lime and ceramic powder in proportion 1:2 and 1:3 by mass.
- By increasing the mixing ratio of ceramic powder/lime up to 3, the percentage of total chemical bound water (attributed to the hydrated products) is augmenting, providing high values of compressive strength and static modulus of elasticity.
- As the ceramic powder/lime ratio increases, the pastes' total cumulative volume and total porosity decrease and a clear shift in pore size distribution curve to narrower pores is observed. The higher percentage of relative volume is distributed in the pore radius between 0.01 and 0.05 μm.

References

1 A. Moropoulou, A. Bakolas and S. Anagnostopoulou, Cem. Concr. Comp., 27 (2005) 295.
2 A. Bakolas, G. Biscontin, A. Moropoulou and E. Zendri, Thermochim. Acta, 321 (1998) 151.
3 R. Bugini, G. Capannesi, C. D'Agostini, C. F. Giulani, A. Salvatori and A. F. Sedda, Proc. Int. Congr. Conservation of Stone and other Materials, Rilem/Unesco, Paris, 1 (1993) 386.
4 H. Boke, S. Akkurt, B. Ipekoglu and E. Ugurlu, Cem. Concr. Res., 36 (2006) 1115.
5 G. Baronio and L. Binda, Constr. Build. Mat., 11 (1997) 41.
6 G. Baronio, L. Binda and N. Lombardini, Constr. Build. Mat., 11 (1997) 33.
7 A. Shvarzman, K. Kovler, G. S. Grader and G. E. Shter, Cem. Concr. Res., 33 (2003) 405.
8 A. Bakolas, E. Aggelakopoulou, S. Anagnostopoulou and A. Moropoulou., J. Therm. Anal. Cal., 84 (2006) 57.
9 S. Salvador, Cem. Concr. Res., 25 (1995) 102.
10 R. A. Livingston, P. E. Stutzman, R. Mark and M. Erdik, Mat. Res. Soc. Symp. Proc., 267 (1992) 721.
11 D. S. Klimesch and A. Ray, Thermochim. Acta, 307 (1997) 167.
12 D. S. Klimesch and A. Ray, Thermochim. Acta, 306 (1997) 159.
13 J. Paya, J. Monzo, M. V. Borrachero, S. Velazquez and M. Bonilla, Cem. Concr. Res., 33 (2003) 1085.
14 J. Pera and A. Amrouz, Adv. Cem. Based Mater., 7 (1998) 49.
15 P. Ubbriaco, P. Bruno, A. Traini and D. Calabrese, J. Therm. Anal. Cal., 66 (2001) 293.

DOI: 10.1007/s10973-007-8858-1